A TRACTION-LAYER MODEL FOR CILIARY PROPULSION

S. R. Keller, T. Y. Wu, and C. Brennen

California Institute of Technology

Pasadena, California

INTRODUCTION

The purpose of this paper is to present a new model for ciliary propulsion intended to rectify certain deficiencies in the existing theoretical models. The envelope model has been developed by several authors including Taylor (1951), Reynolds (1965), Tuck (1968), Blake (1971a, b, c) and Brennen (1974); it employs the concept of representing the ciliary propulsion by a waving material sheet enveloping the tips of the cilia. The principal limitations of this approach, as discussed in the review by Blake and Sleigh (1974), are due to the impermeability and no-slip conditions imposed on the flow at the envelope sheet (an assumption not fully supported by physical observations) and the mathematical necessity of a small amplitude analysis.

In a different approach, Blake (1972) introduced the sub-layer model for evluating the flow within as well as outside the cilia layer by regarding each cilium as an individual slender body attached to an infinite flat plate in a regular array. The flow equations and the no-slip condition at the plate are satisfied by a distribution of Stokes flow force singularities along each cilium. The strength of these singularities is determined by considering the relative velocity between an individual cilium element and an "interaction velocity" which is taken to be the parallel steady flow which the rest of the ciliary array is supposed to create. The resulting complicated integral equations are then solved numerically for the mean velocity profile. As pointed out by Wu (1973) and Brennen (1974), the primary deficiency in the sub-layer model is caused by neglecting the oscillatory component of the "interaction

velocity". From a physical standpoint, since the velocity of the cilia is typically 2 to 3 times the velocity of the mean flow they produce (Sleigh and Aiello (1972)), one might expect the magnitude of the oscillatory velocities to be considerable. Therefore the velocity that each cilium "sees" at any instant during its beat cycle is likely to be quite different from the parallel mean flow alone.

In the traction-layer model developed in this paper, the discrete forces of the cilia ensemble are replaced by an equivalent continuum distribution of an unsteady body force within the cilia layer, and in this discrete-to-continuum force conversion the oscillatory velocities as well as the mean flow are taken into account. Expanding upon the prototype model of Wu (1973), a solution to the fundamental fluid mechanical equations satisfying the appropriate boundary conditions is obtained in terms of an unsteady body force field. This field, which depends upon the movement of the cilia and the "interaction velocity", is meant to be equivalent to the combined effect of the cilia ensemble in generating the resultant flow field. The "interaction velocity", upon which the force field depends, is determined from the instantaneous velocity of the local fluid. The final velocity field is then obtained by a simple and direct numerical iteration of the given solution.

Since in typical organisms the thickness of cilia layer is small compared with the body dimensions, the geometry of the model may be taken as an infinite, flat layer of distributed body force and the cilia are assumed to exhibit planar beat patterns. It has been further demonstrated that flow field solutions for infinite models may be profitably employed as local approximations for finite organisms (see Blake (1973) and Brennen (1974)). Both symplectic and antiplectic metachrony are considered, the extension to other types of metachrony being evident from the discussion.

DESCRIPTION OF THE MODEL

We consider a hypothetical planar organism of infinite extent whose cilia are distributed in a regular array of spacing a in the X direction and b in the Z direction in a Cartesian coordinate system fixed in the organism (see Figure 1). Each cilium is assumed to perform the same periodic beat pattern in an XY plane, with a constant phase difference between adjacent rows of cilia, such that the metachronal wave propagates in the positive X direction.

As already explained, the central concept of this model is to replace the discrete forces of the cilia ensemble by an equivalent continuum distribution of an unsteady body force field $\underline{F}(X, Y, t)$. The vector function $\underline{F}(X, Y, t)$ specifies the instantaneous force

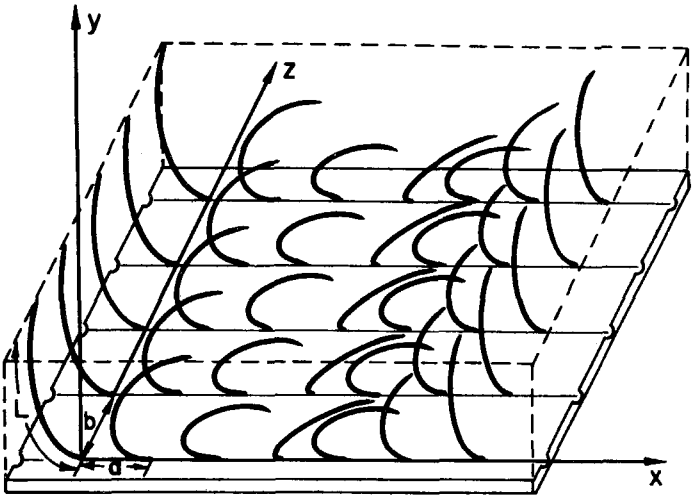

Figure 1. Illustration of the coordinate system and regular array of cilia. The spacing in the X direction is a, while in the Z direction it is b.

acting on a unit element of fluid centered at position (X, Y, Z) and at time t, the fluid element being of unit depth in the Z direction.

For metachronal waves, $\underline{F}$ is a periodic function of $\phi(X, t) = kX-\omega t$, where ω is the angular frequency of the ciliary beat and $k = 2\pi/\lambda$, λ being the metachronal wavelength. Therefore $\underline{F}$ can be expanded in a Fourier series of the form

$$\underline{F}(X, Y, t) = \underline{F}_o(Y) + \sum_{n=1}^{\infty} \mathrm{Re}[\, F_n e^{ni\phi}] \,, \qquad (2.1)$$

where Re stands for the real part, $i = \sqrt{-1}$, and the Fourier coefficients $\underline{F}_n$ $(n \geqslant 1)$ may be complex functions of Y. Further, since the cilia are of finite length L, $\underline{F}$ will vanish above the cilia layer or equivalently

$$F(X, Y, t) = 0 \qquad \text{for } Y > Y_L(kX - \omega t) \qquad (2.2)$$

where $Y = Y_L(kX - \omega t)$ is the thickness of the cilia layer, which depends on $\phi(X, t)$. The Fourier coefficients $\underline{F}_n$ corresponding to the distribution (2.1) will therefore vanish for $Y > L$,

$$\underline{F}_n(Y) = 0 \text{ for } Y > L, \qquad n \geqslant o. \qquad (2.3)$$

SOLUTION OF THE FLUID MECHANICAL PROBLEM

The Navier-Stokes equations for the flow of an incompressible Newtonian fluid in two dimensions may be written as

$$P_X = F + \rho\nu\nabla^2 U - \rho\,(U_t + UU_X + VU_Y) \tag{3.1}$$

$$P_Y = G + \rho\nu\nabla^2 V - \rho\,(V_t + UV_X + VV_Y) \tag{3.2}$$

where P is the pressure, U and V are the X and Y components of velocity respectively, F and G are the X and Y components of body force $\underline{F}$, ρ is the density, and ν the kinematic viscosity. Here and in the sequel, X, Y, and t in subscript denote differentiation. The continuity equation, $U_X + V_Y = 0$, will be satisfied by a stream function Ψ defined by $U = \Psi_Y$, and $V = -\Psi_X$. If we non-dimensionalize all variables using k^{-1}, ω^{-1}, and $\rho\nu k^{-1}\omega^{-1}$ as the reference length, time, and mass scales respectively, the equations of motion in non-dimensional variables (lower case) become

$$p_x = f + \nabla^2\psi_y - R_o(\psi_{y\tau} + \psi_y\psi_{xy} - \psi_x\psi_{yy}) \tag{3.3}$$

$$p_y = g - \nabla^2\psi_x + R_o(\psi_{x\tau} + \psi_y\psi_{xx} - \psi_x\psi_{xy}) \tag{3.4}$$

where $\tau = \omega t$, and $R_o = \omega/\nu k^2$ is the oscillatory Reynolds number which is taken to be much less than unity as is generally the case. The x and y components of equation 2.1, after non-dimensionalization, become

$$f(x, y, t) = f_o(y) + \sum_{n=1}^{\infty} \mathrm{Re}[f_n(y)e^{ni(x-\tau)}] \tag{3.5}$$

$$g(x, y, t) = g_o(y) + \sum_{n=1}^{\infty} \mathrm{Re}[g_n(y)e^{ni(x-\tau)}] \tag{3.6}$$

This suggests that we seek solutions for ψ and p of the form

$$\psi(x, y, \tau) = \psi_o(y) + \sum_{n=1}^{\infty} \mathrm{Re}[\psi_n(y)e^{ni(x-\tau)}] \tag{3.7}$$

$$p(x, y, \tau) = p_o(y) + \sum_{n=1}^{\infty} \mathrm{Re}[\, p_n(y) e^{ni(x-\tau)}] \,. \qquad (3.8)$$

Substituting equations (3.5)-(3.8) into equations (3.3) and (3.4), and equating the appropriate Fourier coefficients, we obtain, after some simplication,

$$(\psi_o)_{yyy} = -f_o + R_o \{1/2 \sum_{n=1}^{\infty} \mathrm{Im}[\, n\psi_n (\bar{\psi}_n)_y]_y\}, \qquad (3.9)$$

$$(p_o)_y = g_o - R_o \{1/2 \sum_{n=1}^{\infty} [\, n^2 \psi_n \bar{\psi}_n]_y\}, \qquad (3.10)$$

$$(\psi_n)_{yyyy} - 2n^2 (\psi_n)_{yy} + n^2 \psi_n = \pi_n + O(R_o), \quad n \geq 1, \qquad (3.11)$$

$$p_n = \frac{1}{ni}[\, f_n + (\psi_n)_{yyy} - n^2 (\psi_n)_y] + O(R_o), \quad n \geq 1, \qquad (3.12)$$

where Im refers to the imaginary part, an overbar signifies the complex conjugate, and $\pi_n = nig_n - (f_n)_y$ $(n \geq 1)$.

The boundary conditions with respect to the reference frame fixed in the organism are as follows. First we impose the no-slip condition at the wall, which requires all the Fourier components of velocity to vanish there, that is

$$(\psi_o)_y(o) = (\psi_n)_y(o) = \psi_n(o) = o, \qquad (n \geq 1). \qquad (3.13)$$

Second, since we are considering an organism which is propelling itself at a constant finite speed, we require that the mean velocity remain bounded while the "AC" components of velocity vanish as $y \to \infty$. Hence

$$(\psi_o)_y(\infty) < \infty, \quad (\psi_n)_y(\infty) = \psi_n(\infty) = o \quad (n \geq 1). \qquad (3.14)$$

Integrating equations (3.9) and (3.10) and applying the boundary conditions (3.13) and (3.14) along with the condition (2.3) yields for the mean velocity and pressure

$$u_o = (\psi_o)_y = \int_o^y y_1 f_o(y_1)dy_1 + y\int_y^{kL} f_o(y_1)dy_1 + R_o\{1/2\sum_{n=1}^{\infty} \mathrm{Im}[\int_o^y n\psi_n(\bar{\psi}_n)_y dy_1]\} \tag{3.15}$$

$$p_o = p_\infty + \int_o^y g_o(y_1)dy_1 - R_o\{1/2\sum_{n=1}^{\infty} n^2\psi_n\bar{\psi}_n\}, \tag{3.16}$$

where p_∞ is an arbitrary constant. Note that as a result of equation (2.3), the zeroth order terms (in R_o) of u_o and p_o are constant for $y = kY > kL$. The first order terms come from the coupling of the "AC" velocities in the nonlinear inertial terms of the fundamental equations. The solution to equation (3.11) subject to equations (3.13), (3.14) and (2.3) is

$$\psi_n = \frac{1}{4n^2}[\alpha_n(y)e^{ny} + \beta_n(y)e^{-ny}] + O(R_o), \text{ where} \tag{3.17}$$

$$\alpha_n(y) = \int_{kL}^{y} (y-y_1-1/n)e^{-ny_1}\pi_n dy_1 \tag{3.18}$$

$$\beta_n(y) = \int_o^y (y-y_1+1/n)e^{ny_1}\pi_n dy_1 - \int_o^{kL} (y+y_1+2nyy_1+1/n)e^{-ny_1}\pi_n dy_1 . \tag{3.19}$$

The harmonic x and y velocities, $u_n = \mathrm{Re}[(\psi_n)_y e^{ni(x-\tau)}]$ and $v_n = -\mathrm{Re}[ni\psi_n e^{ni(x-\tau)}]$, $n \geq 1$, decay like e^{-ny}. The dimensional velocities U_n and V_n are obtained by simply multiplying u_n and v_n by $c = \omega/k$, the wave speed. The solution for the harmonic pressure coefficients may be determined from equations (3.12) and (3.17) directly.

Finally we observe that for the cilia layer to be self-propelling the condition of zero mean longitudinal force acting on the organism can be expressed by

$$\mu \frac{\partial U_o(o)}{\partial Y} = \int_o^L F_o(y_1) dy_1 , \tag{3.20}$$

where $\mu = \rho\nu$ is the dynamic viscosity coefficient; the mean shearing force exerted by the fluid on the wall balances the mean force per unit area of the organism's surface due to the reaction of the fluid to the ciliary body force field. It is of interest to note that the present solution, given by equations (3.15)-(3.19), automatically satisfies condition (3.20) required for self-propulsion when the mean force $\underline{F}_o(y)$ of the ciliary layer is regarded as known. This is in effect a consequence of the boundary condition imposed at infinity, as Taylor (1951) pointed out. To an observer in a frame fixed with the fluid at infinity (the lab frame), the organism is moving with a constant velocity and hence, by conservation of momentum, must have zero net force acting on it.

FORCE EXERTED BY A CILIUM

In the preceding section the solution to the fluid mechanical problem was given as if the body force field $\underline{F}$ were known a priori. Since in practice this is not the case, we need to develop a means of determining $\underline{F}$. As an initial step in this regard, we consider the force exerted on the fluid by a single cilium.

In order to calculate the viscous force exerted by an elongated cylindrical body moving through a viscous fluid, it is convenient to utilize the simple approximations of slender-body resistive theory. If the tangential and normal velocities relative to the local fluid of a cylindrical body element of length ds are $\underline{V}_s$ and $\underline{V}_n$ respectively, the tangential force exerted by the body element on the viscous fluid will be $d\underline{F}_s = C_s \underline{V}_s ds$ with a similar expression for the normal force $d\underline{F}_n = C_n \underline{V}_n ds$, where C_s and C_n are the corresponding resistive force coefficients.

The expressions for the force coefficients have received considerable attention by several authors. The original expressions given by Gray and Hancock (1955) were for an infinitely long circular cylinder moving in an unbounded fluid. Cox (1970) developed slightly modified coefficients to account for other simple shapes. Recent work by Katz and Blake (1974) have yielded improved coefficients for slender bodies undergoing small amplitude normal motions near a wall. For the purposes of the present investigation, however, initially, the force coefficients developed by Chwang and Wu (1975) for a very thin ellipsoid of semi-major axis $\frac{1}{2}L$, and semi-minor axis r_o are used. These are defined by

$$C_n = \frac{4\pi\mu}{\ln(L/r_o) + \frac{1}{2}} \quad \text{and} \quad C_s = \frac{2\pi\mu}{\ln(L/r_o) - \frac{1}{2}} \,. \tag{4.1}$$

If we describe the motion of a single cilium with base fixed at the origin by a parametric position vector $\underline{\xi}(s,t)$ specifying the position of the element ds of the cilium identified by the arc length s at time t, then the force exerted by the element ds on the fluid is given by

$$d\underline{F}_c = C_s[\,\gamma(\underline{\xi}_t - \underline{U}) + (1-\gamma)\underline{\xi}_s(\underline{\xi}_t - \underline{U})\cdot\underline{\xi}_s\,]\,ds\,, \tag{4.2}$$

where $\underline{U}$ is the local fluid velocity, which is inter-related to F_c, and $\gamma = C_n/C_s$. In the formula above $\partial\underline{\xi}/\partial t$ provides the velocity of motion of the cilium element at s and $\partial\underline{\xi}/\partial s$ signifies the unit vector tangential to the longitudinal curve of the cilium centroid. We are thus left with the task of evaluating $\underline{F}_c$ and then converting it to the body force field.

DETERMINATION OF THE BODY FORCE FIELD

In order to apply the resistive theory in determining the body force field $\underline{F}$, two difficulties must be overcome. Equation (4.2) describes the force exerted by an element as a function of its arc length s. It is convenient to convert this Lagrangian description of the force to Eulerian coordinates (i.e. to express the force as a function of X and Y). In addition, the force exerted by an element depends upon the local fluid velocity, which is initially unknown. Both of these features suggest a numerical iteration approach.

While a detailed description of the numerical approach is beyond the scope of this paper, a brief account of the scheme will be given. From equation (2.1) it follows that

$$F_o = 1/\lambda\int_o^\lambda F(X,Y,t_o)dX, \quad F_n = 2/\lambda\int_o^\lambda F(X,Y,t_o)e^{-ni\phi}dX \tag{5.1}$$

$(n \geq 1)$

This implies that if the body force field were known over one wavelength for some (arbitrary) fixed time t_o, then all the force coefficients could be determined. In order to accomplish this for a given ciliary beat pattern, an analytical representation for $\underline{\xi}(s,t)$ can be determined using a finite Fourier series-least

square procedure. (For the details of this procedure see Blake (1972)). Thus the movement of a single cilium is given by

$$\underline{\xi}(s,t) = 1/2\, a_o(s) + \sum_{n=1-n}^{N} a\ (s)\cos n\omega t + b_n(s)\sin n\omega t, \qquad (5.2)$$

where $\underline{a}_n(s) = \sum_{n=1}^{M} \underline{A}_{mn} s^m$, $\underline{b}_n(s) = \sum_{n=1}^{M} \underline{B}_{mn} s^m$, with $\underline{A}_{mn}$ and $\underline{B}_{mn}$ being constant vectors.

Once $\underline{\xi}(s,t)$ is determined, an initial body force field can be established via a "pigeon-hole"algorithm. Using equation (5.2), the cilia are numerically distributed over one wavelength at a fixed time t_o and each cilium is broken up into a finite number of segments. The Eulerian location of and the force exerted by each segment are then determined and stored (i.e. "pigeon-holed"). The force is evaluated using equation (4.2) initially with $\underline{U}$, the local fluid velocity, equal to zero. The zpproximation is made that the force exerted by each segment is located at the midpoint of that segment, so that the force field can be represented by the expression

$$F(X,Y,t_o) = 1/b \sum_{j=1}^{J} \underline{f}_j \delta(X-X_j)\delta(Y-Y_j), \qquad (5.3)$$

where $\underline{f}_j$ is the force exerted by the j-th ciliary segment whose midpoint is located at (X_j, Y_j) and J is the total number of segments in one wavelength. The factor $1/b$ is to account for averaging in the Z direction.

Calculations of the body force field can then be carried out by iteration. Equation (5.3) is used in equation (5.1) to determine the Fourier force coefficients $\underline{F}_n$ $(n \geqslant o)$. These coefficients, after non-dimensionalization, are then used in equations (3.15) and (3.17) to determine a new local velocity field $\underline{U}$. This velocity field is used anew in the pigeon-hole algorithm to determine a new $\underline{F}(X,Y,t_o)$ by computing new $\underline{f}_j$'s. The iterative process is thus repeated until the $\underline{f}_j$'s, and hence the velocity field $\underline{U}$, converges.

RESULTS

Preliminary calculations have been carried out on data obtained for Opalina ranarum and Paramecium multimicronucleatum. Although these two organisms have been observed to have somewhat three dimensional beat patterns, they were chosen because

of the availability of the necessary data and for comparison with previous theoretical work. The raw planar beat patterns were taken from Sleigh (1968) and Figure 2 shows the results of the Fourier series - least squares procedure (see equation (5.2)) with $M = N = 3$ for Opalina and $M = N = 4$ for Paramecium. The metachrony of Opalina is symplectic, while Paramecium was regarded as exhibiting antiplectic metachrony, although it recently has been reported to be dexioplectic (Machemer (1972)).

In order to display the harmonic X-velocity components, it is convenient to write them in the form

$$U_n = Q_n \cos(n\phi + \theta_n), \quad (n \geq 1), \text{ where} \tag{6.1}$$

$$Q_n = c\,|\psi_{n\,y}|\,, \text{ and} \tag{6.2}$$

$$\theta_n = \tan^{-1}[\,\mathrm{Im}(\psi_{n\,y})/\mathrm{Re}(\psi_{n\,y})] \tag{6.3}$$

For a given value of Y, Q_n is the amplitude of the nth harmonic X-velocity component, while θ_n is the phase of the motion. This phase is such that U_n is at a maximum and in the same direction as the mean flow when $\phi = (2\ell\pi - \theta_n)/n$, while U_n is at a maximum and opposes the mean flow when $\phi = [\,(2\ell-1)\pi - \theta_n]\,/n$, where ℓ is an integer.

In performing the computations, besides the basic beat pattern, it was necessary to specify the three dimensionless parameters ka, kb, and kL. The values of the parameters were chosen to be consistent with the consensus of experimental observations (see e.g. Blake and Sleigh (1974) and Brennen (1974)). The values used for ka and kb were 0.63 and 0.13 for Opalina and 0.80 and 1.60 for Paramecium. Two values of the amplitude parameters kL, to which the computations were the most sensitive, were used for each organism, these being 1.25 and 2.50 for Opalina and 3.00 and 6.00 for Paramecium. Because of the apparent rapid decay of the higher harmonics and for computational efficiency, only the first harmonic was retained in computing the local velocity field U in three cases, however, the second harmonic was included for Paramecium with kL = 3.00.

Figures 3 and 4 show the velocity profiles for U_0, the mean fluid velocity parallel to the wall, for Opalina and Paramecium respectively. Also plotted are the profiles given by Blake (1972) (dashed curve). The velocities at infinity, U^∞/c, which correspond to the velocities of propulsion, are seen to agree quite well with the observed values of 0.5-1.5 for Opalina and 1-4 for Paramecium (Brennen (1974)). Blake's calculations were made

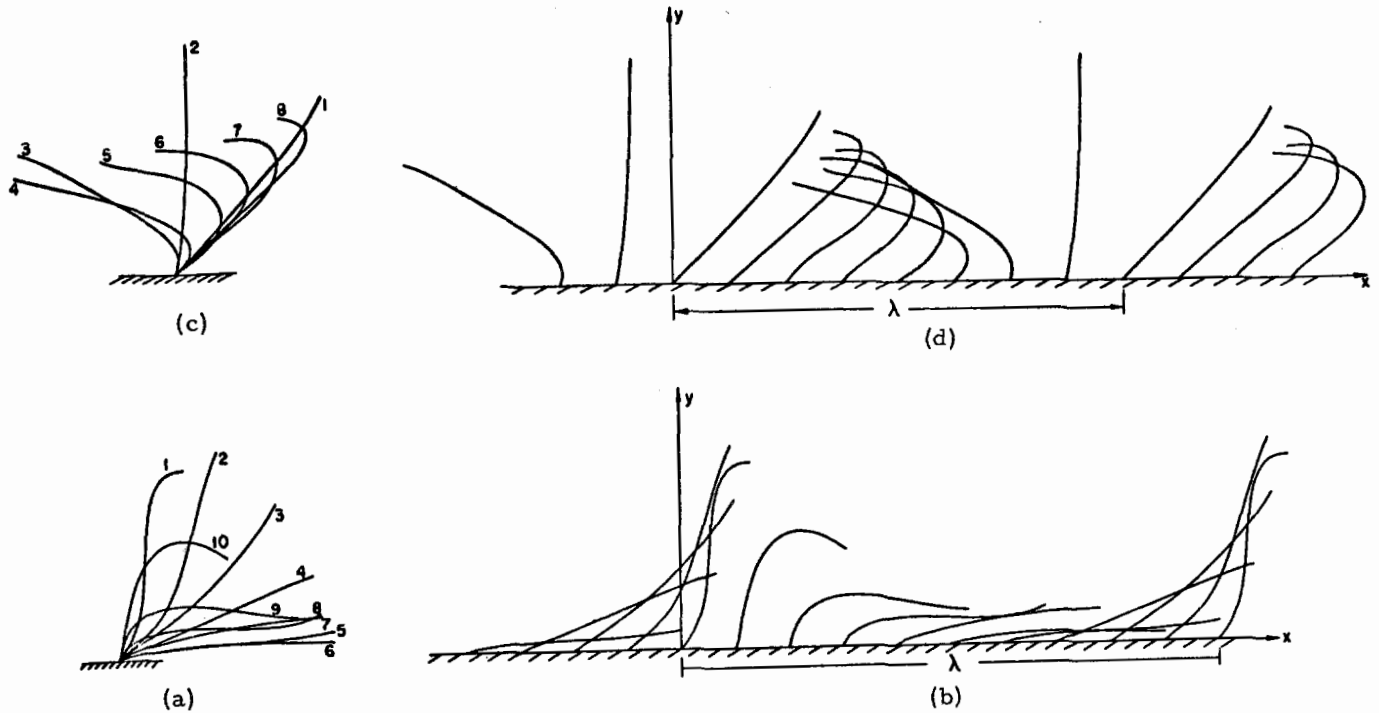

Figure 2. Plots of the analytical representation of the beat patterns for Opalina (a, b) and Paramecium (c, d). Numbers indicate successive equal time increments of the beat cycle. The movement of an individual cilium is shown in (a) and (c), while (b) and (d) represent a "snapshot" of the cilia at $t = t_o$.

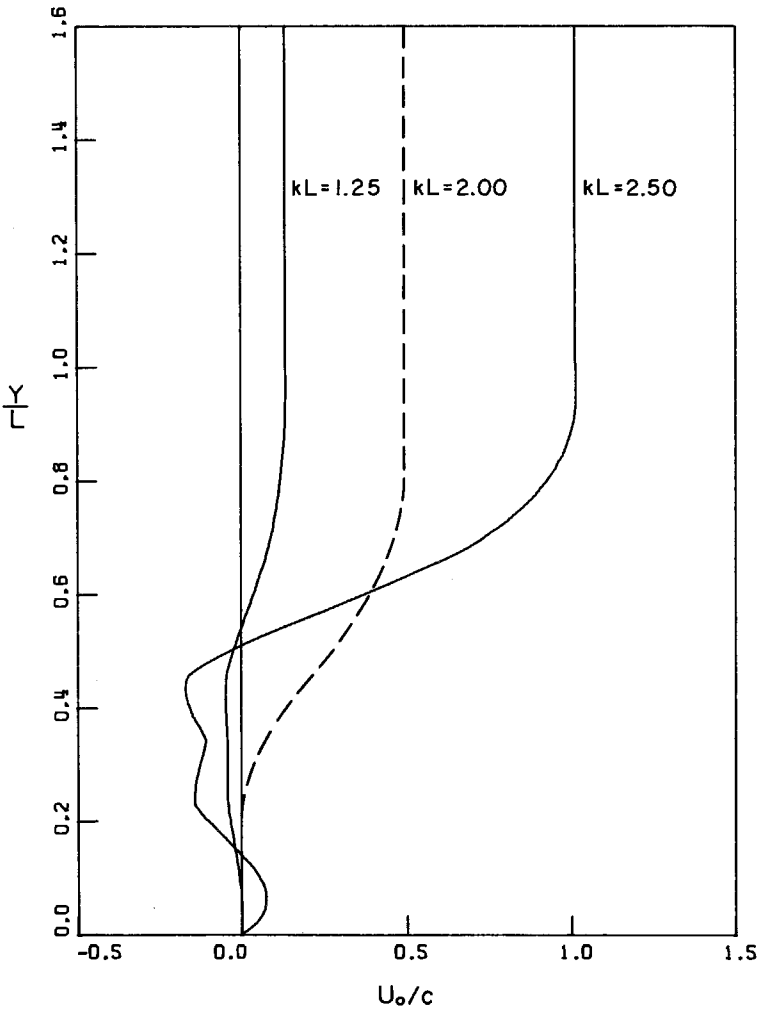

Figure 3. Mean velocity profiles for Opalina with ka = 0.63 and kb = 0.13. Dashed curve is from Blake (1972) for which (ka)(kb) = 0.04.

with the quantity (ka)(kb) equal to 0.04 for Opalina and 0.00025 for Paramecium (both far below the reported values) so that a direct comparison is difficult. While Blake's results indicate a slight backflow for only the antiplectic case, the present study indicates a backflow in the lower half of the cilia layer for both Opalina and Paramecium (for kL = 6).

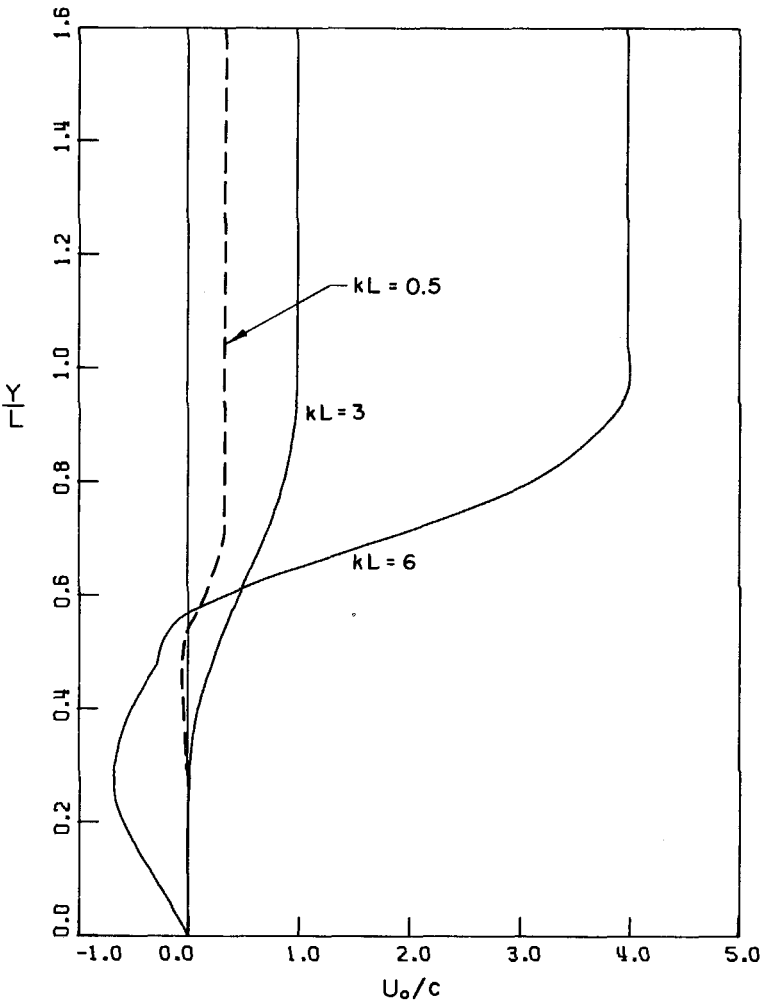

Figure 4. Mean velocity profiles for Paramecium with ka = 0.80 and kb = 1.60. Dashed curve is from Blake (1972) for which (ka)(kb) = 0.00025.

Figure 5 shows the amplitude of the first harmonic velocity component U_1 for Opalina. The largest oscillatory velocities appear to occur at $Y/L = 6$ and are more than twice the mean flow in magnitude. In Figure 6 the amplitudes of U_1 for kL equal 3 and 6 and U_2 for kL equal 3 are shown for Paramecium. The largest oscillatory velocities occur in the upper part of the cilia layer and are about the same magnitude as the mean flow. Note that for kL = 3 the amplitude of U_2 is half that of U_1.

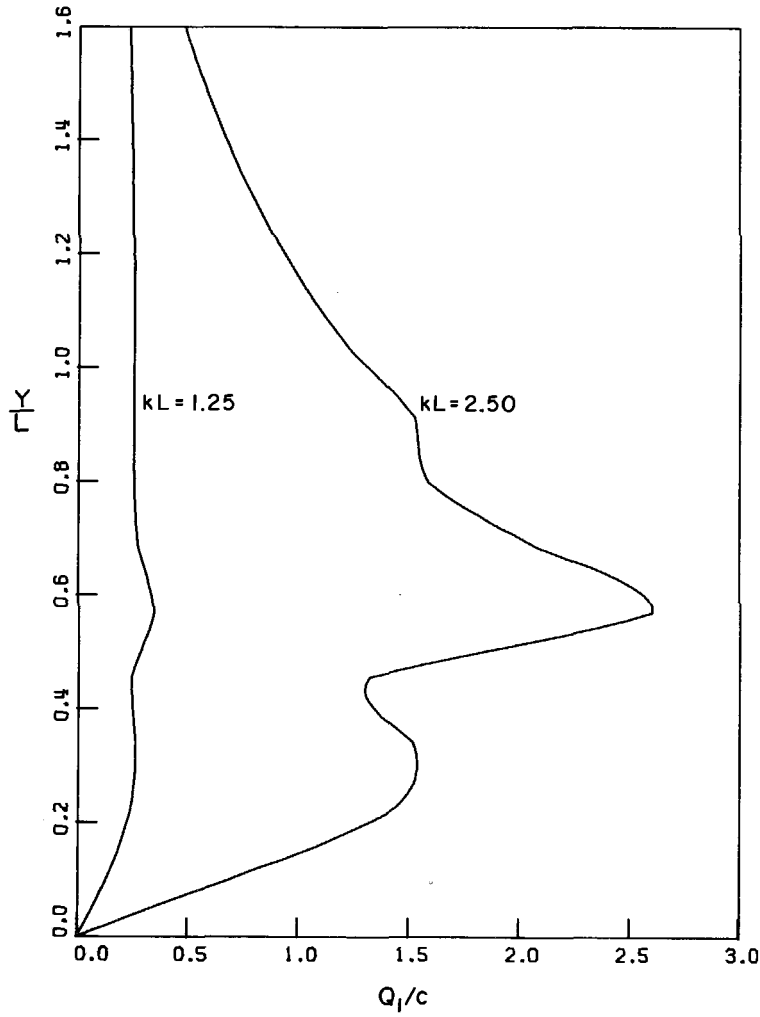

Figure 5. Amplitude profile for the first harmonic X-velocity component for Opalina with ka = 0.63 and kb = 0.13.

The corresponding θ_n's for Figures 5 and 6 are shown in Figures 7 and 8 respectively. The origin and the value of t_o (see the previous section) were chosen so that $\phi = 0$ corresponds to a metachronal wave peak under which the cilia are in the effective stroke. This is illustrated in Figure 2 which can be regarded as a snapshot of the cilia at $t = t_o$. For Opalina at $Y/L = 0.5$ and $\phi = 0$, $U_1/Q_1 = \cos(\theta_1)$ equals approximately 1 for $kL = 1.25$ and 0 for $kL = 2.5$. This means that U_1 is somewhat in the same direction as the mean flow in the vicinity of the cilia

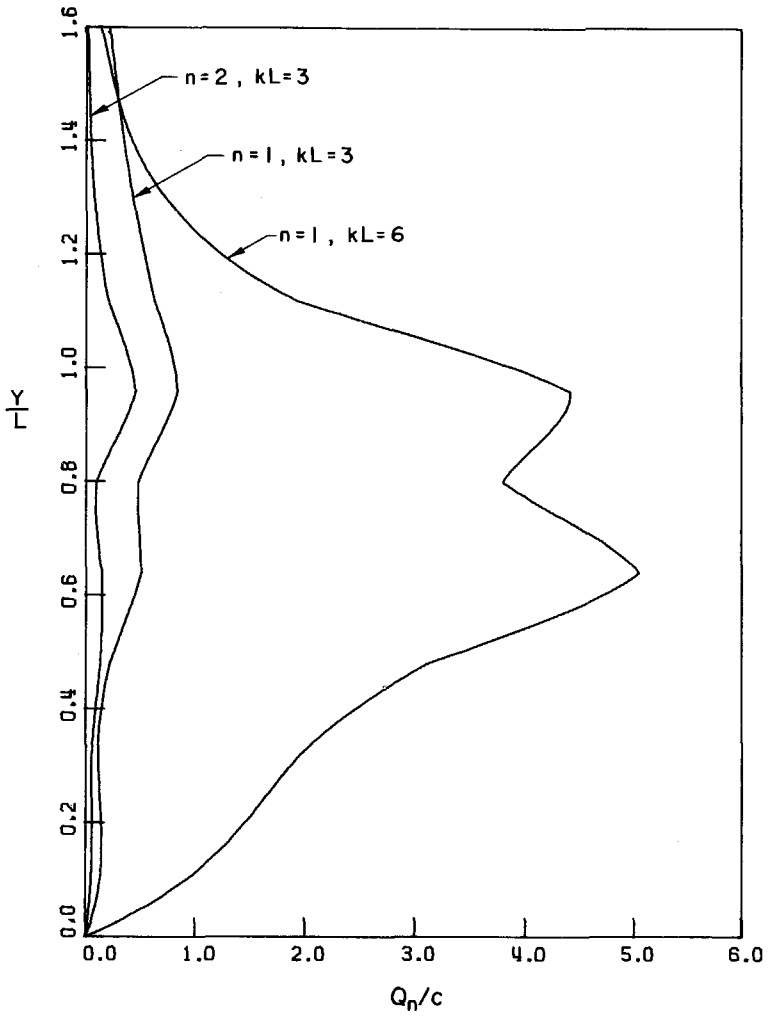

Figure 6. Amplitude profiles for n^{th} harmonic X-velocity components for Paramecium with ka = 0.80 and kb = 1.60.

performing the effective stroke. However, above Y/L = 0.5 U_1 progressively tends to oppose the mean flow. For Paramecium however, at Y/L = 0.5 and ϕ = 0, U_1/Q_1 equals -1 for both kL values. Thus, in this case, U_1 tends to oppose the mean flow in the vicinity of the effective stroke. It is also seen that U_2 (for kL = 3) is in the same direction as the mean flow near the effective stroke (ϕ = 0) for much of the cilia layer.

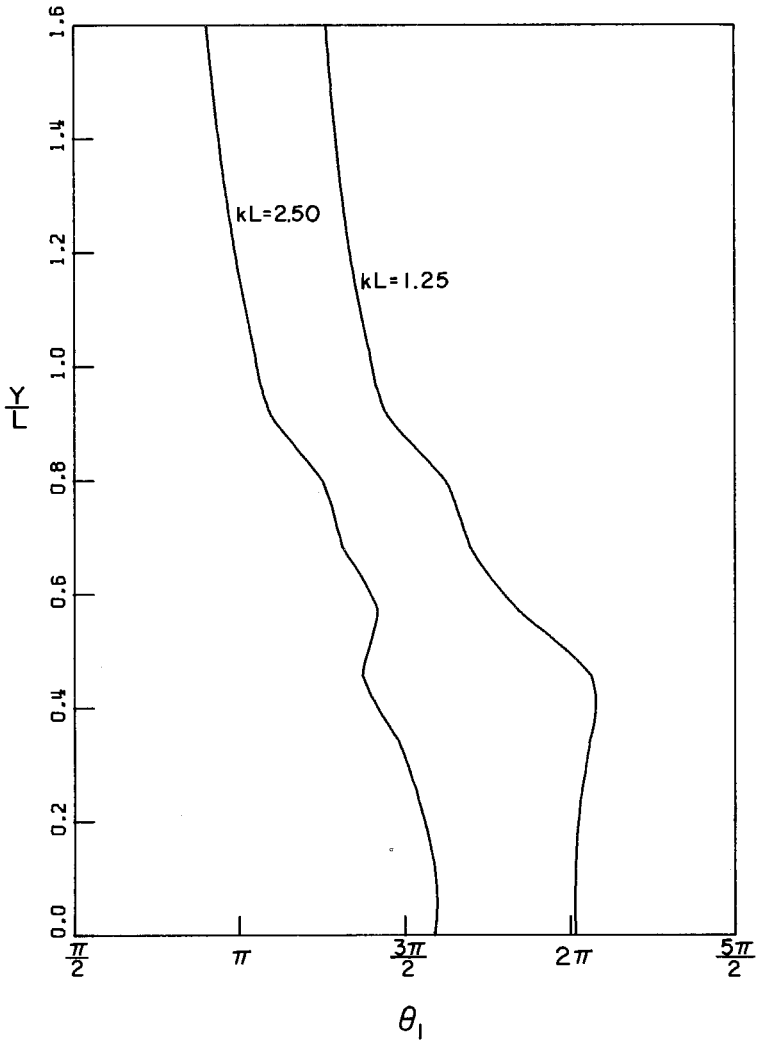

Figure 7. Variation of θ_1, the phase of the first harmonic X-velocity component, with Y/L for Opalina.

SUMMARY

The main features of the model developed in this paper are that it allows for the large amplitude motion of cilia and takes into account the oscillatory aspects of the flow. When applied to Opalina and Paramecium, a good agreement is found between theoretically predicted and experimentally observed velocities of propulsion. The amplitude of the oscillatory velocities is found

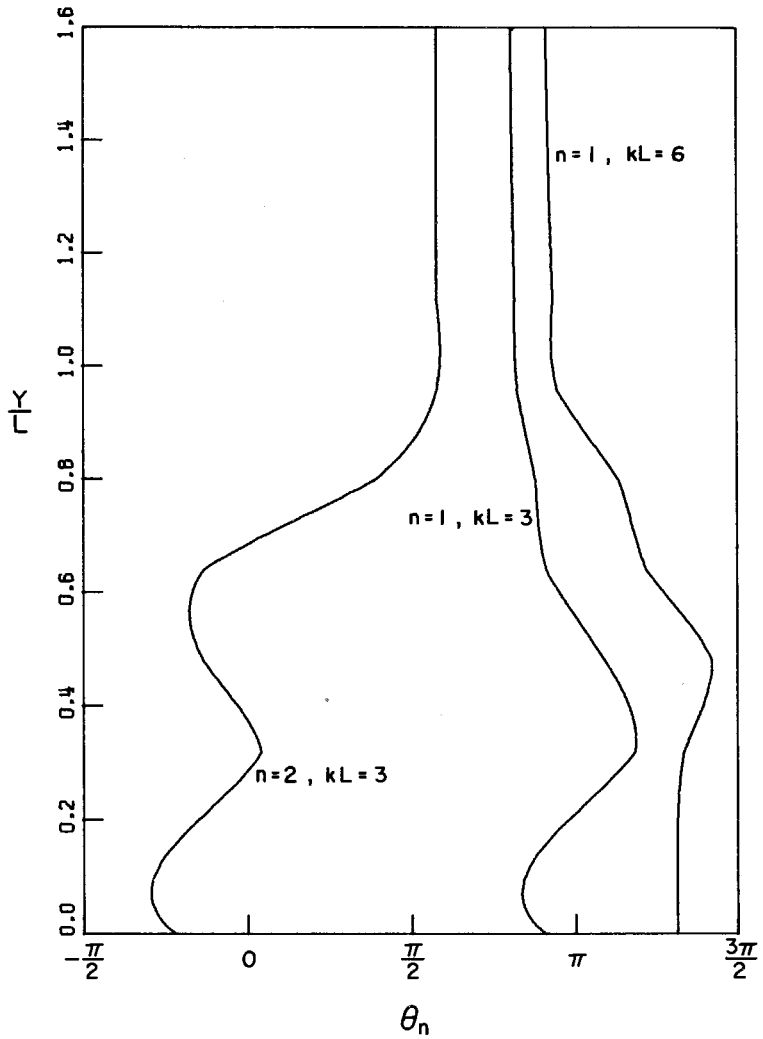

Figure 8. Variation of θ_n, the phase of the n^{th} harmonic X-velocity component, with Y/L for Paramecium.

to be of the same order of magnitude as the mean flow within the cilia layer and to decay exponentially outside the cilia layer.

ACKNOWLEDGMENT

This work was jointly sponsored by the National Science Foundation and by the Office of Naval Research.

REFERENCES

Blake, J.R. 1971a A spherical envelope approach to ciliary propulsion. J. Fluid Mech. 46, 199-208.

Blake, J.R. 1971b Infinite models for ciliary propulsion. J. Fluid Mech. 49, 209-222.

Blake, J.R. 1971c Self-propulsion due to oscillations on the surface of a cylinder at low Reynolds number. Bull. Aust. Math. Soc. 5, 255-264.

Blake, J.R. 1972 A model for the micro-structure in ciliated organisms. J. Fluid Mech. 55, 1-23.

Blake, J.R. 1973 A finite model for ciliated micro-organisms. J. Biomech. 6, 133-140.

Blake, J.R. and Sleigh, M.A. 1974 Mechanics of ciliary locomotion. Biol. Rev. 49, 85-125.

Brennen, C. 1974 An oscillating-boundary-layer theory for ciliary propulsion. J. Fluid Mech. 65, 799-824.

Chwang, A.T. and Wu, T.Y. 1975 Hydrodynamics of the low-Reynold-number flows. Part 2. The singularity method for Stokes flows. J. Fluid Mech. 67, 787-815.

Cox, R.G. 1970 The motion of long slender bodies in a viscous fluid. Part 1. General theory. J. Fluid Mech. 44, 791-810.

Gray, J. and Hancock, G.J. 1955 The propulsion of sea-urchin spermatozoa. J. exp. Biol. 32, 802-814.

Katz, D.F. and Blake, J.R. 1974 Flagellar motions near a wall. Proceedings of the Symposium on Swimming and Flying in Nature, Pasadena, California, July 8-12.

Machemer, H. 1972 Ciliary activity and origin of metachrony in Paramecium: Effects of increased viscosity. J. exp. Biol. 57, 239-259.

Reynolds, A.J. 1965 The swimming of minute organisms. J. Fluid Mech. 23, 241-260.

Sleigh, M.A. 1968 Patterns of ciliary beating. Symp. Soc. exp. Biol. 22, 131-150.

Sleigh, M.A. and Aiello, E. 1972 The movement of water by cilia. Acta. Protozool. 11, 265-277.

Taylor, G. I. 1951 Analysis of swimming microscopic organisms. Proc. R. Soc. Lond. A. 209, 447-461.

Tuck, E. O. 1968 A note on a swimming problem. J. Fluid Mech. 31, 305-308.

Wu, T. Y. 1973 Fluid mechanics of ciliary propulsion. Proceedings of the Tenth Anniversary Meeting of the Society of Engineering Science. (in press).